Journal of Chromatography, 644 (1993) 231–238
Elsevier Science Publishers B.V., Amsterdam

CHROM. 25 185

Studies on a new cross-axis coil planet centrifuge for performing counter-current chromatography

II. Path and acceleration of coils and comparison with type J coil planet centrifuge

Jean-Michel Menet[☆] and Yoichiro Ito*

Laboratory of Biophysical Chemistry, National Heart, Lung, and Blood Institute, National Institutes of Health, Building 10, Room 7N322, Bethesda, MD 20892 (USA)

(First received November 24th, 1992; revised manuscript received March 30th, 1993)

ABSTRACT

A comprehensive approach is introduced using parametric equations to describe the motion induced by type J and cross-axis type coil planet centrifuges. The plots of a line parallel to the coil axis are given. The centrifugal forces are then analyzed in two ways. Three-dimensional graphs show their geometry and the relative intensity of the lateral component is compared to that of the perpendicular component. This allowed a better understanding of the differences in paths and acceleration fields induced by the two types of counter-current chromatography devices.

INTRODUCTION

Type J [1] and cross-axis type [2] coil planet centrifuges (CPCs) induce motions that are best studied using parametric equations. Since the global motions are separated, they allow a better comprehension of the resulting path. The parametric equations for the motion of a point belonging to the column are given as well as those for its acceleration. The β parameter [3], the ratio of the coil radius to the radius of rotation for the coil holder, is then introduced for both units. The path of a line, parallel to the axis of the coil, is shown for type J CPC and cross-axis CPC equipped with coils in various positions. The plots allow examination of the influence of β on the shape of the paths.

Two procedures are applied to study the accelerations. First, the use of parametric definitions provides simple plots of their three-dimensional geometry. Alternatively perpendicular and lateral components of the total acceleration are considered relative to the axis of the tube.

Both procedures show the complexity of the acceleration field for type J CPC and the important role of the lateral component of the acceleration. The L position (central position of the coil) on the cross-axis CPC shows a simpler acceleration field while the lateral component remains small compared to the perpendicular acceleration. The $X-1.5L$ position (off-center position) on the cross-axis CPC involves a quite complex acceleration field, leading to a particu-

* Corresponding author.
☆ Guest scientist from Laboratoire de Chimie Analytique, Ecole Supérieure de Physique et de Chimie Industrielles de Paris, 10 Rue Vauquelin, 75231 Paris Cedex 05, France.

0021-9673/93/$06.00

larly important lateral component of the total acceleration.

APPARATUS

Two classical CPCs are studied using our theoretical investigations. One is a Type J CPC from P.C. Inc. (Potomac, MD, USA). Its planetary motion has been widely described in the literature [1].

The other one is the fifth cross-axis prototype; its mechanical principle has been described in Part I [4]. The coil is made of a thin polytetrafluoroethylene (PTFE) tube wound directly onto a cylinder, whose axis is horizontal. This column is mounted in a holder, turning around the central (vertical) axis of the apparatus. Coils of two diameters were used. The holder was designed to accommodate the column in a central position (its axis cuts off the central axis of the CPC), named L, or the off-center position, named $X-1.5L$.

The main geometrical characteristics of the two devices are gathered in Table I.

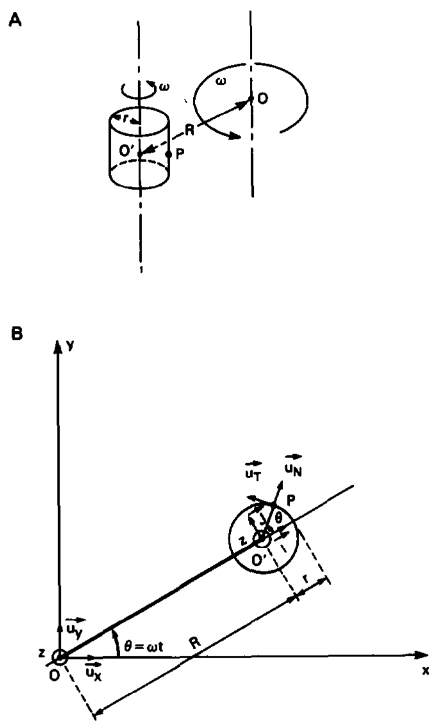

Fig. 1. Type J motion. (A) Principle; (B) mathematical study.

TABLE I

GEOMETRICAL CHARACTERISTICS AND MAXIMUM CENTRIFUGAL FORCE INTENSITIES FOR TWO COUNTER-CURRENT CHROMATOGRAPHY (CCC) DEVICES: TYPE J CPC UNIT AND CROSS-AXIS PROTOTYPE

n.d. = Not defined.

CCC device	Type J CCC	Cross-axis CCC			
		L position		$X-1.5L$ position	
r (mm)	$58.0<r<87.0$	27.5	50.0	27.5	50.0
R (mm)	101.5	0	0	104	104
L (mm)	n.d.	168.6	168.6	168.6	168.6
β	$0.55<\beta<0.77$	0.16	0.30	0.26	0.48
θ_0 (°)	n.d.	0	0	31.7	31.7
ω (rpm)	750	800	800	800	800
Maximum number of gravities obtained	280	160	195	180	250

THEORY

All the calculations for the type J CPC have previously been made for the path and acceleration [5]. However, the goal here is to separate the global motion into elementary motions in order to provide better understanding of the results. These procedures are applied below to type J CPC, yielding the results previously computed and the same technique is also applied to the cross-axis type CPC.

Type J synchronous coil planet centrifuge

Analysis of the path. The motion can be studied with a three-dimensional coordinate system $O;\vec{u}_x,\vec{u}_y,\vec{u}_z$ named (R). This system is considered as the motionless reference system. Another coordinate system $O';\vec{I},\vec{J},\vec{u}_z$ named (R') is also introduced. O′ is a point undergoing a circular motion around the z axis with radius R at a constant angular velocity ω. The principle of type J motion is explained in Fig. 1A and all the notations used for the mathematical studies are shown in Fig. 1B. The circular motion of O′ is described in the (R) system by the parametric equations:

$$\overrightarrow{OO'} = \left| \begin{array}{ll} R\cos(\omega t) & \vec{u}_x \\ R\sin(\omega t) & \vec{u}_y \\ 0 & \vec{u}_z \end{array} \right. \qquad (1)$$

Let us consider an arbitrary point P, belonging to the column. Its motion in the (R') system is a circle of radius r, in the O; $\vec{I}$, $\vec{J}$ plane, with an ω angular velocity around the z axis. The parametric equations are:

$$\overrightarrow{O'P} = \left| \begin{array}{ll} r\cos(\omega t) & \vec{I} \\ r\sin(\omega t) & \vec{J} \\ 0 & \vec{u}_z \end{array} \right. \qquad (2)$$

Then these equations are given in the (R) system:

$$\overrightarrow{OP} = \left| \begin{array}{ll} R\cos(\omega t) + r\cos(2\omega t) & \vec{u}_x \\ R\sin(\omega t) + r\sin(2\omega t) & \vec{u}_y \\ 0 & \vec{u}_z \end{array} \right. \qquad (3)$$

The β ratio, equal to r/R, is introduced, leading to

$$\overrightarrow{OP} = R \left| \begin{array}{ll} \cos(\omega t) + \beta\cos(2\omega t) & \vec{u}_x \\ \sin(\omega t) + \beta\sin(2\omega t) & \vec{u}_y \\ 0 & \vec{u}_z \end{array} \right. \qquad (4)$$

Analysis of the acceleration. The acceleration, defined in the (R) system by:

$$\overrightarrow{a(P)} = \frac{d^2\overrightarrow{OP}}{dt^2} \qquad (5)$$

is then written in the (R) coordinate system:

$$\overrightarrow{a(P)} = -R\omega^2 \left| \begin{array}{ll} \cos(\omega t) + 4\beta\cos(2\omega t) & \vec{u}_x \\ \sin(\omega t) + 4\beta\sin(2\omega t) & \vec{u}_y \\ 0 & \vec{u}_z \end{array} \right. \qquad (6)$$

Cross-axis synchronous coil planet centrifuge

Analysis of the path. Two coordinate systems are used. $O;\vec{u}_x,\vec{u}_y,\vec{u}_z$ named (R) and $O';\vec{I},\vec{J},\vec{u}_z$

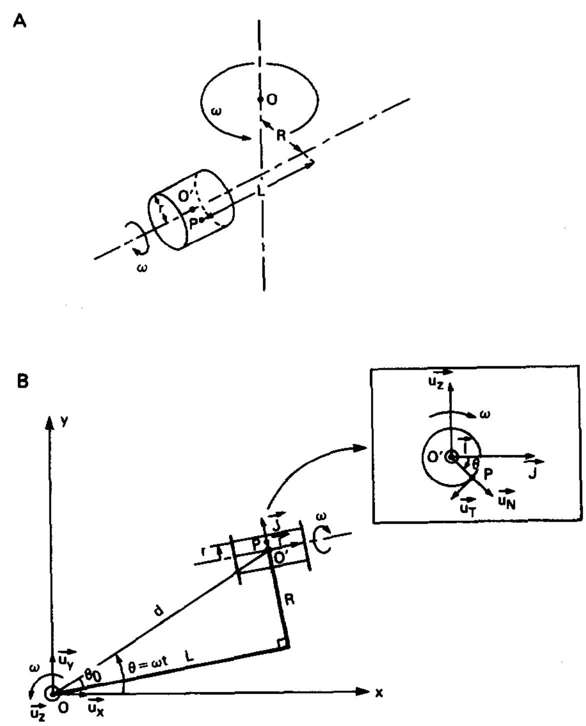

Fig. 2. Cross-axis type motion. (A) Principle; (B) mathematical study.

named (R') were previously defined. O' is a point undergoing a circular motion around the z axis with radius d at a constant angular velocity ω. The principle of cross-axis type motion is explained in Fig. 2A. Fig. 2B gives all the notations used for the following studies. The length d is computed as $d=\sqrt{R^2+L^2}$ and angle θ_0 is defined by $\tan\theta_0=R/L$. The circular motion of O' is described in the (R) system by the parametric equations:

$$\overrightarrow{OO'}\left|\begin{array}{ll} d\cos(\omega t) & \vec{u}_x \\ d\sin(\omega t) & \vec{u}_y \\ 0 & \vec{u}_z \end{array}\right. \quad (7)$$

Let us consider an arbitrary point P, belonging to the column. Its motion in the (R') system is a circle of radius r, in the $O';\vec{J},\vec{K}$ plane, with an ω angular velocity around the $O';\vec{I}$ axis. The parametric equations are:

$$\overrightarrow{O'P}=\left|\begin{array}{ll} 0 & \vec{I} \\ r\cos(\omega t) & \vec{J} \\ -r\sin(\omega t) & \vec{u}_z \end{array}\right. \quad (8)$$

Then these equations are given in the (R) system:

$$\overrightarrow{OP}\left|\begin{array}{ll} d\cos(\omega t)-r\cos(\omega t)\sin(\omega t-\theta_0) & \vec{u}_x \\ d\sin(\omega t)+r\cos(\omega t)\cos(\omega t-\theta_0) & \vec{u}_y \\ -r\sin(\omega t) & \vec{u}_z \end{array}\right. \quad (9)$$

Analysis of the acceleration. Using the relation 5 in the (R) system, the acceleration is written:

$$\overrightarrow{a(P)}=-\omega^2\left|\begin{array}{ll} d\cos(\omega t)-2r\sin(2\omega t-\theta_0) & \vec{u}_x \\ d\sin(\omega t)+2r\cos(2\omega t-\theta_0) & \vec{u}_y \\ -r\sin(\omega t) & \vec{u}_z \end{array}\right. \quad (10)$$

TABLE II

PARAMETRIC EQUATIONS DESCRIBING THE POSITION OF A POINT BELONGING TO THE COLUMN AND ITS ACCELERATION FOR TYPE J AND CROSS-AXIS CPCs

β is defined as $\beta=r/R$, except for the L-position for which $\beta=r/L$.

	Column position	$\vec{OP}$	$\vec{a}(P)$
Type J CPC	Not defined	$R\left\|\begin{array}{l}\cos(\omega t)+\beta\cos(2\omega t)\\ \sin(\omega t)+\beta\sin(2\omega t)\\ 0\end{array}\right.$	$-R\omega^2\left\|\begin{array}{l}\cos(\omega t)+4\beta\cos(2\omega t)\\ \sin(\omega t)+4\beta\sin(2\omega t)\\ 0\end{array}\right.$
	L	$L\left\|\begin{array}{l}\cos(\omega t)-\beta\sin(\omega t)\cos(\omega t)\\ \sin(\omega t)+\beta\cos^2(\omega t)\\ -\beta\sin(\omega t)\end{array}\right.$	$-L\omega^2\left\|\begin{array}{l}\cos(\omega t)-2\beta\sin(2\omega t)\\ \sin(\omega t)+2\beta\cos(2\omega t)\\ -\beta\sin(\omega t)\end{array}\right.$
Cross-axis CPC	$X-LL$	$\frac{L}{2}\left\|\begin{array}{l}\sqrt{5}\cos(\omega t)-\beta\sin(\omega t-\theta_0)\cos(\omega t)\\ \sqrt{5}\sin(\omega t)+\beta\cos(\omega t)\cos(\omega t-\theta_0)\\ -\beta\sin(\omega t)\end{array}\right.$	$\frac{-L\omega^2}{2}\left\|\begin{array}{l}\sqrt{5}\cos(\omega t)-2\beta\sin(2\omega t-\theta_0)\\ \sqrt{5}\sin(\omega t)+2\beta\cos(2\omega t-\theta_0)\\ -\beta\sin(\omega t)\end{array}\right.$
	$X-L$	$L\left\|\begin{array}{l}\sqrt{2}\cos(\omega t)-\beta\sin(\omega t-\pi/4)\cos(\omega t)\\ \sqrt{2}\sin(\omega t)+\beta\cos(\omega t)\cos(\omega t-\pi/4)\\ -\beta\sin(\omega t)\end{array}\right.$	$-L\omega^2\left\|\begin{array}{l}\sqrt{2}\cos(\omega t)-2\beta\sin(2\omega t-\pi/4)\\ \sqrt{2}\sin(\omega t)+2\beta\cos(2\omega t-\pi/4)\\ -\beta\sin(\omega t)\end{array}\right.$
	General	$\left\|\begin{array}{l}d\cos(\omega t)-r\cos(\omega t)\sin(\omega t-\theta_0)\\ d\sin(\omega t)+r\cos(\omega t)\cos(\omega t-\theta_0)\\ -r\sin(\omega t)\end{array}\right.$	$-\omega^2\left\|\begin{array}{l}d\cos(\omega t)-2r\sin(2\omega t-\theta_0)\\ d\sin(\omega t)+2r\cos(2\omega t-\theta_0)\\ -r\sin(\omega t)\end{array}\right.$

Three positions of the coil were then studied. The notations were defined by Ito [6]. The L position corresponds to $R = 0$, leading to $d = L$ and $\theta_0 = 0$. The $X - L$ position corresponds to $R = L$, leading to $d = \sqrt{2}R$ and $\theta_0 = \pi/4$. The $X - LL$ position is defined by $L = 2R$ and leads to $d = \sqrt{5}R$ and θ_0 defined by $\tan \theta_0 = 1/2$. Table II gathers all the parametric equations for type J CPC and cross-axis CPC involving a coil in three different positions, L, $X - L$ and $X - LL$. Type J equations were previously given in formulas 4 and 6, and general equations for cross-axis type were also obtained in formulas 9 and 10. The equations for the L, $X - L$ and $X - LL$ positions are derived from the general ones, using their geometric characteristics.

RESULTS AND DISCUSSION

All the equations given in Table II allow three-dimensional plots of paths of points or accelerations. In order to better understand the motions induced by the two CPCs, we studied the paths of a line drawn on the coil, parallel to the axis of the latter. The accelerations of one point were also studied.

Analysis of the path

All the equations given in Table II involve the β ratio as a key parameter. Selected values were then used to plot the paths for a line drawn along the axis of the coil, for type J CPC and cross-axis type CPC, with a coil in L, $X - L$ or $X - LL$ position. The shapes of the paths are all shown in Fig. 3. The individual paths of five points were plotted, allowing display of the path of the interconnecting straight line parallel to the axis of the coil.

For type J CPC, the shapes of the path are greatly dependent on β [7]. They are only two-dimensional, in the xy plane. For small β ($\beta < 0.25$), the path is quite circular, but slightly flattened. For $\beta = 0.25$, the shape becomes cycloidal. For $0.25 < \beta < 0.25$, the cycloidal path is more pronounced. β values greater than 0.5 involve an inner loop, whose size increases with β.

The shapes for the three positions L, $X - L$ and $X - LL$ of the cross-axis CPC are very similar. All are three-dimensional. For small β values ($\beta < 0.4$), the shape is again simple resembling a circle, with a small component on the vertical axis Oz. As the β value increases ($0.4 \leqslant \beta \leqslant 0.5$), a deformation occurs near the Oy axis, and at larger β values, this deformation evolves from a "drop" of the path near the Oy axis to a loop. The latter is shown for each of the three positions when the radius of the coil is twice the radius R.

These studies can be applied to the two CPCs described in part Apparatus. The type J device involves β values greater than 0.5; consequently, the path always shows a loop. The cross-axis prototype shows more simple paths, quite circular with a small component on the vertical axis. No loop intervenes as the radii of the coils are small compared to the R radius.

Analysis of the acceleration

The following explanations refer to the force field which is opposite to the acceleration field. Two different studies were carried out. First, the geometric characteristics of the centrifugal force fields were considered. The influence of the β ratio has revealed to be important for the force field created by the type J motion [8]. Therefore, five plots are shown in Fig. 4, drawn in the xy plane. For $\beta = 0.1$, the shape of the path is quite circular, and the corresponding force field is similar to that obtained with a completely circular motion. The direction of the force is almost perpendicular to the path and the variations in intensity are small. Where $\beta = 0.2$, a modification is seen near the Ox axis: the relative intensity of the lateral component of the centrifugal force field increases while the total intensity of this latter greatly diminishes. For $\beta = 0.25$, the total intensity becomes equal to 0 on the Ox axis. For higher β values, the centrifugal force field never cancels, but the relative intensity of the lateral force becomes very important near the loop. The influence of β for the centrifugal force field created by the cross-axis CPC is less important than for the type J CPC. Four plots are given in Fig. 5. Fig. 5A corresponds to the L position of the coil with $\beta = 0.5$ and two plots are necessary to represent the force field, since it is three-dimensional. The

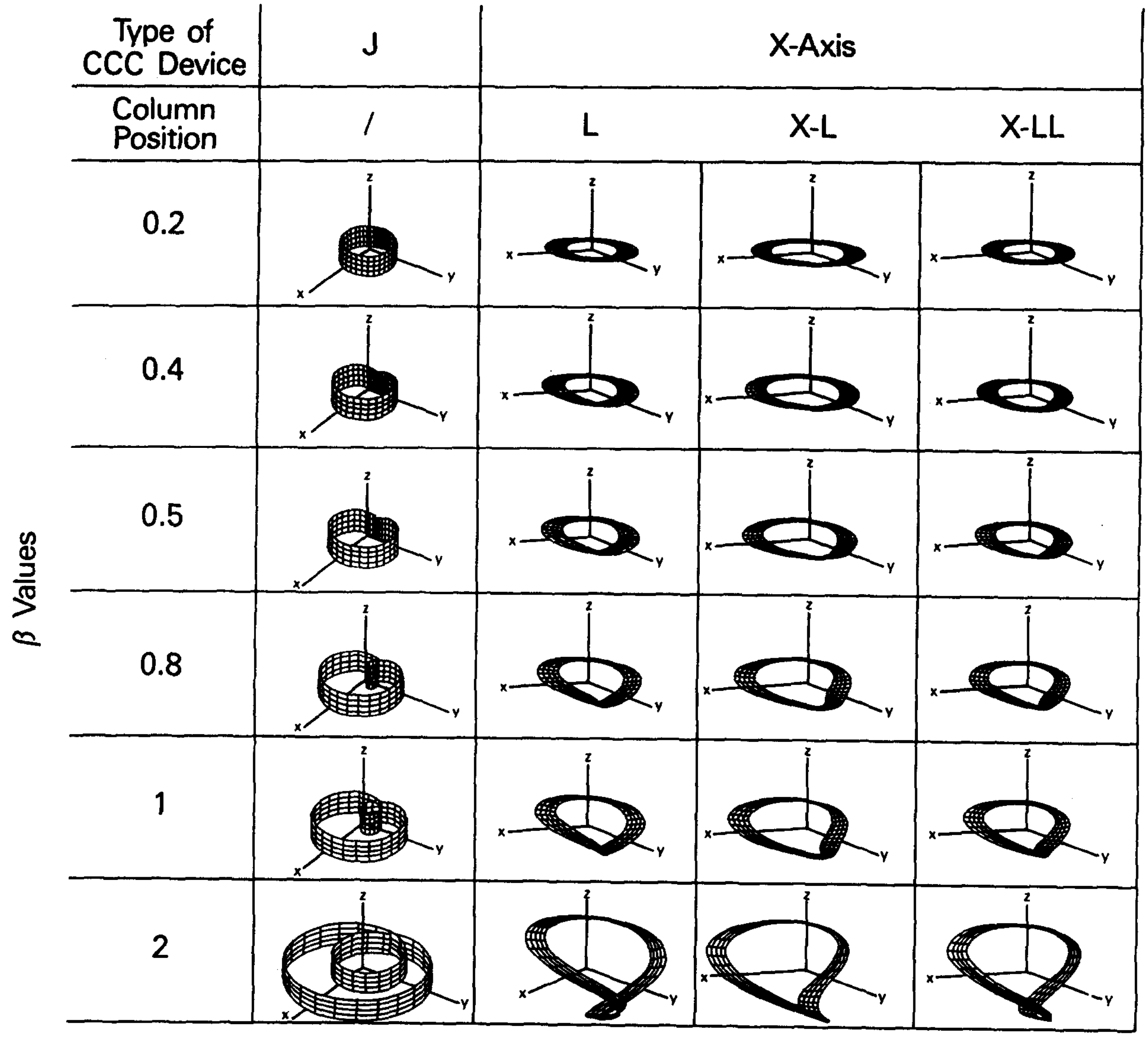

Fig. 3. Paths of a line drawn along the axis of the coil belonging to a type J CPC or a cross-axis (X-axis) CPC; influence of the β ratio and of the position of the coil for a cross-axis CPC.

centrifugal field in the xy plane (Fig. 5A, 1) is similar to that obtained with type J motion for $\beta = 0.25$, but it never cancels completely. Its projection in the xz plane is shown in Fig. 5A, 2. Fig. 5B refers to the $X-L$ position of the coil with $\beta = 0.5$. The projections in the xy and xz planes are given in Fig. 5B, 1 and 2. The geometry of the centrifugal force field appears similar to that for the L position of the coil, as the axis of symmetry in the xy plane is no longer Oy but a line defined by the θ_0 angle.

The second set of studies was done to examine the influence of the total centrifugal acceleration by analyzing its tangential (lateral) and normal (perpendicular) components. For both CPCs, the direction perpendicular to the tube is given by vector $\overrightarrow{O'P}$ (see Figs. 1 and 2). The corre-

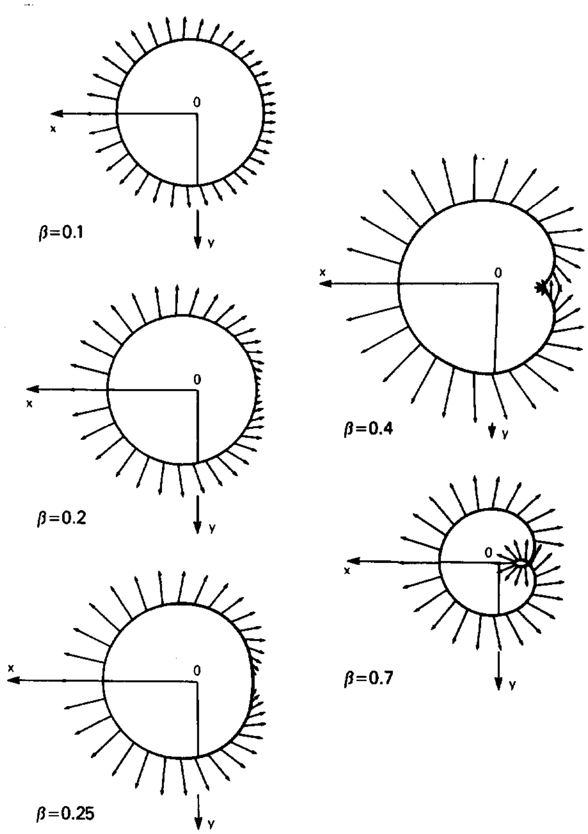

Fig. 4. Type J CCC unit: relative magnitude and direction of the centrifugal force field at various angles along the path of a point. Influence of β.

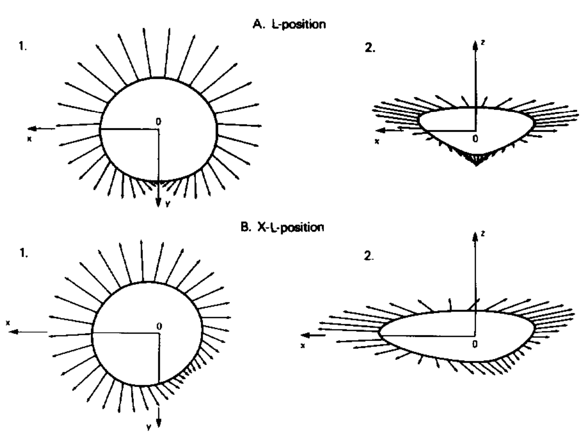

Fig. 5. Cross-axis CCC unit: relative magnitude and direction of the centrifugal force field at various angles along the path of a point. (A) L Position; (B) $X-L$ position.

sponding normalized vectors $\vec{u}_T$ and $\vec{u}_N$ are computed in the (R') coordinate system. For type J CPC, using the acceleration of point P, $\overrightarrow{a(P)}$, given in formula 6 and rewritten in the (R') system, its tangential component a_T and normal component a_N are computed as:

$$\begin{cases} a_T = \overrightarrow{a(P)} \cdot \vec{u}_T = R\omega^2 \sin(\omega t) \\ a_N = \overrightarrow{a(P)} \cdot \vec{u}_N = -R\omega^2[\cos(\omega t) + 4\beta] \end{cases} \tag{11}$$

For the type J apparatus (P.C. Inc.), $\beta > 0.25$; consequently, the term $\cos(\omega t) + 4\beta$ remains always positive. The normal component of the acceleration is thus always directed toward the interior of the coil. Except for two angular positions, which lead to $\sin(\omega t) = 0$, a lateral component is involved but is always smaller than a_T. The maximum relative intensity of the lateral acceleration is obtained when $\sin(\omega t) = 1$, resulting in $a_T/a_N = 1/4\beta$. Using the smaller β values of the type J CPC, this ratio is equal to 0.45, which indicates the tangential acceleration represents up to 45% of the normal acceleration. For the first half of the path $(0 < \theta < 180°)$, $\vec{u}_T$ and the lateral force have opposite directions, although for the second half of the path $(180 < \theta < 360°)$, their directions are the same. The influence of that change of direction is more important for $\theta \approx 180°$ because the normal force is smaller than that corresponding to $\theta \approx 0°$, thus increasing the relative importance of the tangential force. This could be related to the settling zone around $\theta = 0°$ and the mixing zone around $\theta = 180°$, as described by Conway and Ito from stroboscopic observations [9].

The same studies apply to the cross-axis prototype. Using the acceleration of point P, $\overrightarrow{a(P)}$, given in formula 10 and rewritten in the (R') system, its tangential component a_T, normal component a_N and component a_I on the O'; $\vec{I}$ axis are computed as:

$$\begin{cases} a_I = \overrightarrow{a(P)} \cdot \vec{I} = -L\omega^2 + 2r\omega^2 \sin(\omega t) \\ a_T = \overrightarrow{a(P)} \cdot \vec{u}_T = \omega^2 \sin(\omega t)[R + r\cos(\omega t)] \\ a_N = \overrightarrow{a(P)} \cdot \vec{u}_N = -r\omega^2 - \cos(\omega t)\omega^2[R + r\cos(\omega t)] \end{cases} \tag{12}$$

These expressions can be simplified for the L position and lead to:

$$\begin{cases} a_{\mathrm{I}} = r\omega^2\left[2\sin(\omega t) - \frac{L}{r}\right] \\ a_{\mathrm{T}} = r\omega^2 \sin(\omega t)\cos(\omega t) \\ a_{\mathrm{N}} = -r\omega^2\left[\cos^2(\omega t) + 1\right] \end{cases} \quad (13)$$

In that case, it is easy to study the relative intensities of the three components of the total acceleration. The geometrical dimensions of the cross-axis prototype with a coil in the L position (see Table I) are introduced in formula 13. Examination of the ratio $a_{\mathrm{T}}/(\sqrt{a_{\mathrm{I}}^2 + a_{\mathrm{N}}^2})$ demonstrates that the tangential component represents up to 16.5% of the total normal component for the larger radius ($r = 50.0$ mm); it can represent up to 9% for the smaller radius ($r = 27.5$ mm). Consequently, the total centrifugal force acting on the fluids inside the tube involves three forces: two are perpendicular to the tube, directed toward the outside; the third is parallel to the axis of the tube, acting with a small intensity (a maximum 16.5% of the gathered two perpendicular forces for the 50.0 mm coil radius) and changing direction four times during one turn of the central axis of the device. Whereas type J CPC involves a maximum 280 g centrifugal force and a lateral force representing up to 45% of the perpendicular force, the lateral force for the cross-axis proptotype using a coil in the L position is three times smaller and the maximum centrifugal force is 195 g. The position $X - 1.5L$ was also studied as the geometrical characteristics of the cross-axis prototype (given in Table I) are introduced in formula 12. Whatever the radius of the coil may be (2.75 cm or 5.0 cm), a_{I} is always negative, a_{T} has the sign of $\sin(\omega t)$ and a_{N} is positive or negative. Analysis of the ratio $a_{\mathrm{T}}/(\sqrt{a_{\mathrm{I}}^2 + a_{\mathrm{N}}^2})$ allowed estimation of the relative intensity of the lateral force compared to the centrifugal force exerted perpendicularly to the axis of the tube. For the small radius ($r = 2.75$ cm), the maximum for the ratio is 0.9 and the larger radius ($r = 5.0$ cm) can lead to 1.25.

CONCLUSIONS

The results demonstrate that the two CCC types create different force fields. The type J CPC induces a loop for β larger than 0.25, leading to a specific force field. The intensity of the lateral component of the acceleration may represent one half of the component perpendicular to the axis of the tube. For the cross-axis CPC, the positions of the coil lead to similar paths but different acceleration characteristics. The L position induces mainly an acceleration perpendicular to the tube, with a small lateral component representing a maximum of one sixth of the total intensity of the forces perpendicular to the tube. The $X - 1.5L$ position greatly increases the role of the lateral force, whose intensity can be larger than that of the total perpendicular centrifugal force.

Further investigations will be necessary to correlate these acceleration studies with the observed retention of the stationary phase related to the position of the coil and the direction of elution or the elution mode. The use of four two-phase solvent systems and statistical analysis should help in this goal. In the following article (Part III [10]), retention data of the four two-solvent systems are analysed by reference to these studies.

REFERENCES

1 Y. Ito, in N.B. Mandava and Y. Ito (Editors), *Countercurrent Chromatography—Theory and Practice*, Marcel Dekker, New York, 1988, Ch. 3, p. 422.
2 Y. Ito, *Sep. Sci. Technol.*, 22 (1987) 1971.
3 Y. Ito, in N.B. Mandava and Y. Ito (Editors), *Countercurrent Chromatography—Theory and Practice*, Marcel Dekker, New York, 1988, Ch. 3, p. 333.
4 K. Shinomiya, J.-M. Menet, H.M. Fales and Y. Ito, *J. Chromatogr.*, 644 (1993) 215.
5 W.D. Conway, *Countercurrent Chromatography—Apparatus, Theory and Applications*, VCH, New York, 1990, pp. 128–136.
6 Y. Ito, E. Kitazume, M. Bhatnagar and F. Trimble, *J. Chromatogr.*, 538 (1991) 59.
7 W.D. Conway, *Countercurrent Chromatography—Apparatus, Theory and Applications*, VCH, New York, 1990, p. 130.
8 W.D. Conway, *Countercurrent Chromatography—Apparatus, Theory and Applications*, VCH, New York, 1990, p. 135.
9 W.D. Conway and Y. Ito, presented at the *Pittsburgh Conference, Atlantic City, NJ, March 1984.*
10 J.-M. Menet, K. Shinomiya and Y. Ito, *J. Chromatogr.*, 644 (1993) 239.